Journal of the Korean Physical Society, Vol. 54, No. 1, January 2009, pp. 355∼360

Development of a Water-Window X-ray Source Using a Liquid-Nitrogen Jet

B. Ahn and J. Kim
Vacuum and Measurement Technology, Pohang 790-320

J. Son, B. Kim and D. Kim*
Department of Physics, Pohang University of Science and Technology, Pohang 790-784

(Received 21 August 2007)

As a source for a soft X-ray microscope, a liquid-nitrogen jet has been developed and its radiation characteristics have been investigated for various laser parameters, such as the laser pulse energy and duration. The effects of pre-pulse and multiple pulses have also been studied. The focus has been the N VI $1s2$-$1s2p$ transition at 2.88 nm. The investigation shows that the laser intensity for the maximum conversion efficiency scales as $I_m \propto 1/\tau^{\alpha}$, where $\alpha = 0.9 \pm 0.15$. The study of the pre-pulse effect on the conversion efficiency shows that a pre-pulse of only 2 mJ enhances the conversion efficiency by 10 – 15 times for the main pulse of 15 – 60 mJ at a delay of 3 – 6 ns. The photon flux is 1.2×10^{12} photons / (pulse sr) at a delay of 4 ns for a main pulse of 60 mJ with a pre-pulse of 4 – 8 mJ. The study of the multiple pulse effect was done in the 4-pulse configuration. The enhancement of the radiation compared to the accumulation of the radiation intensity of each pulse was observed at a certain delays between 4 pulses, implying that there exists a proper pulse structure for maximum radiation.

PACS numbers: 52.38.Ph, 52.38.Mf, 52.50.Jm
Keywords: Water window, Liquid nitrogen jet

I. INTRODUCTION

Laser-produced plasmas have become excellent compact short-wavelength sources for various purposes [1–6]. A laser-produced plasma is a suitable compact X-ray source that can be broad band or quasi-monochromatic with a proper choice of material and filter. If an efficient source is to be made, the condition for maximum conversion efficiency at a desired wavelength should be found [7–9]. The desired wavelength varies, depending on an application. For example, 13-nm radiation is needed for extreme ultraviolet (EUV) lithography, the water-window radiation (2.3 – 4.4 nm) for soft X-ray microscopy and the hard X-ray radiation for medical imaging.

In this paper, we present the development of a liquid-nitrogen jet and its radiation characteristics for different laser parameters and the effect of many pulses on the radiation output. Section II discusses the liquid-nitrogen jet and its basic radiation characteristics and the effect of the pre-pulse added to the main pulse is presented in Section III. The effect of more than 2 pulses is discussed in Section IV.

*E-mail: kimd@postech.ac.kr

II. WATER-WINDOW RADIATION FROM A LIQUID-NITROGEN JET

To be a suitable source for a water-window X-ray high-resolution microscope, the source has to meet the following three conditions: 1) have monochromatic radiation in the water-window, 2) have strong intensity of radiation and 3) be debris free. A liquid-nitrogen jet satisfies all theses conditions. The N VI $1s2$-$1s2p$ transition at 2.88 nm is very strong. The density of liquid nitrogen is close to the solid density. Since nitrogen is a gas at room temperature, liquid nitrogen evaporates after its interaction with a laser, producing no debris.

This motivation has driven us to develop a liquid-nitrogen jet system. A high-purity and high-pressure nitrogen gas was fed into a gas line and then into a capillary with a tapered nozzle at the other end. The nitrogen gas was cooled and liquefied by using two liquid-nitrogen cooling stages. Especially, the first cooling stage further removes residual water vapor in the nitrogen gas. This removal is important to form a stable liquid jet for a long duration because tiny ice pieces from water vapor may block the nozzle. The liquid-nitrogen was then injected into a vacuum chamber through a capillary nozzle. For a stable jet, the nozzle has to be tapered. The tapering of a nozzle with an angle of at least larger than 15° is

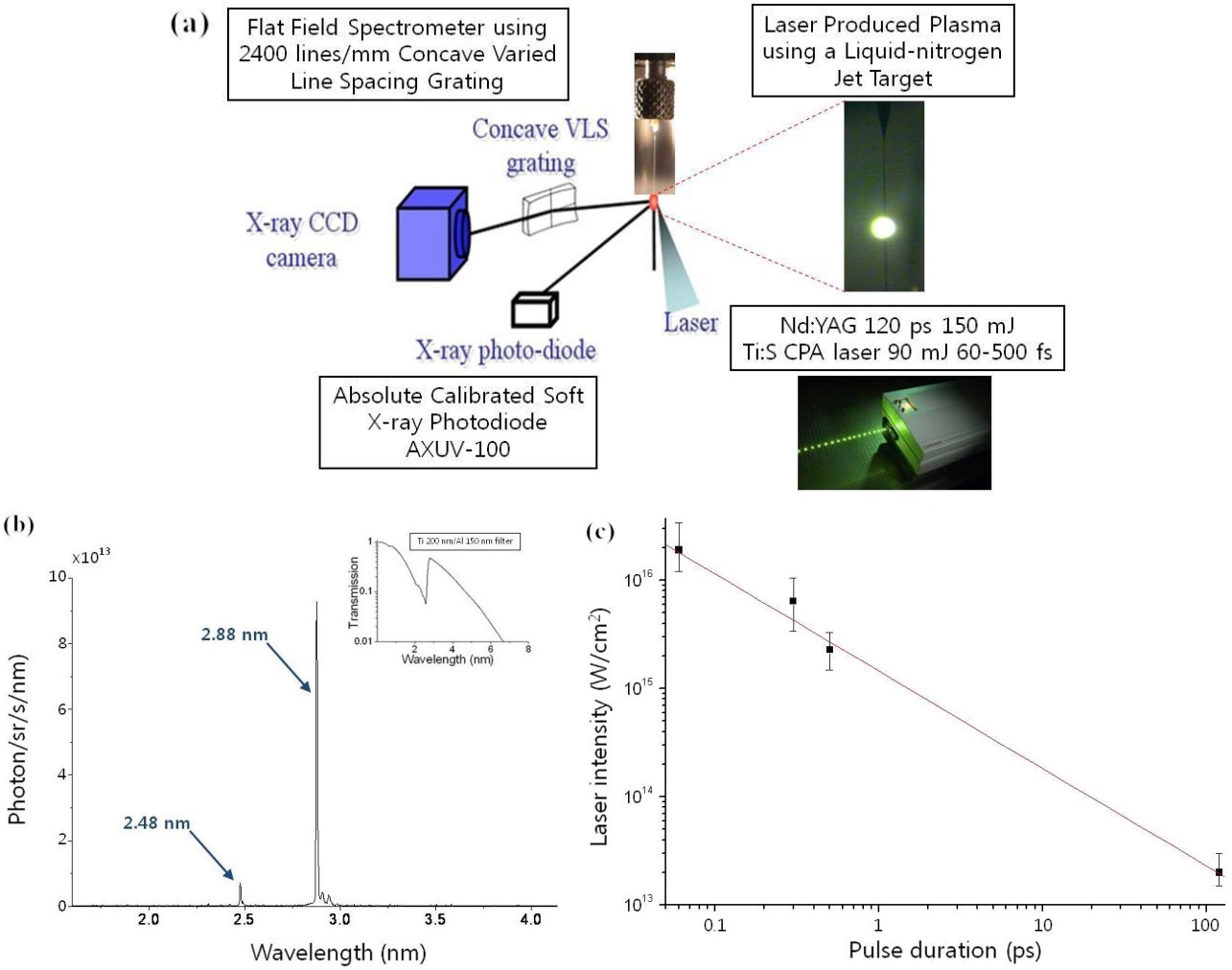

Fig. 1. (a) Experimental setup for a water-window source using a liquid-nitrogen jet target. (b) Spectrum in the water-window region produced from liquid nitrogen at a laser intensity of 1.5×10^{14} W/cm^2 from a 120-ps pulsed Nd:YAG laser. A Ti 200 nm/Al 150 nm filter was used for the quasi-monochromatic spectrum. The inset is the transmission curve of the filter. (c) The laser intensity of the maximum conversion efficiency vs the pulse duration.

recommended [10]. We used a nozzle with a tapering angle of 20°. The backing pressure and the nozzle diameter are also important factors for stable operation. The investigation tells us that a backing pressure of 0.5 – 3.0 MPa for a 10- to 30-μm-diameter nozzle is a suitable condition for a stable liquid-nitrogen jet. It is so stable that it vibrates less than 2 μm. By increasing the backing pressure, the stable region can be extended to several millimeters at the cost of the vacuum. A higher pumping speed is needed to maintain a vacuum of a few mTorr. The data presented below were obtained using a nozzle with a diameter of 12 or 13 μm. The diameter of the formed jet was about 10 μm.

The experimental apparatuses used in this study are shown schematically in Figure 1(a). Two different high-power laser systems were used in this work. The first one is a Nd:YAG laser at 532 nm at 10 Hz, whose pulse duration is 120 ps and whose maximum energy is 150 mJ/ pulse. The other one is a Ti:S laser at 10 Hz that has a tunable pulse duration from 40 to 500 fs and a maximum energy of 90 mJ/ pulse. The pulse width is controlled by using the grating separation in the compressor. A f = 150-mm lens was used for the Nd:YAG laser and a f = 200-mm lens for the femtosecond laser. The focal spot size measured was about 20 μm in diameter for both lasers. A flat field spectrometer (FFS) and an absolutely calibrated X-ray photodiode [11] were used to characterize the radiations. The FFS is equipped with a 2400 line/mm grating and a soft X-ray CCD. Figure 1(b) shows a typical quasi-monochromatic spectrum obtained with a Ti 200 nm/Al 150 nm filter (the inset shows the transmission of the filter). The strong single line is the N VI $1s2$-$1s2p$ transition at 2.88 nm and the weak one is the N VII $1s$-$2p$ transition at 2.48 nm. The absolute intensity of 4×10^{11} photons / (pulse sr) at 2.88 nm was obtained for a 120-ps, 532-nm laser at 1.5×10^{14}

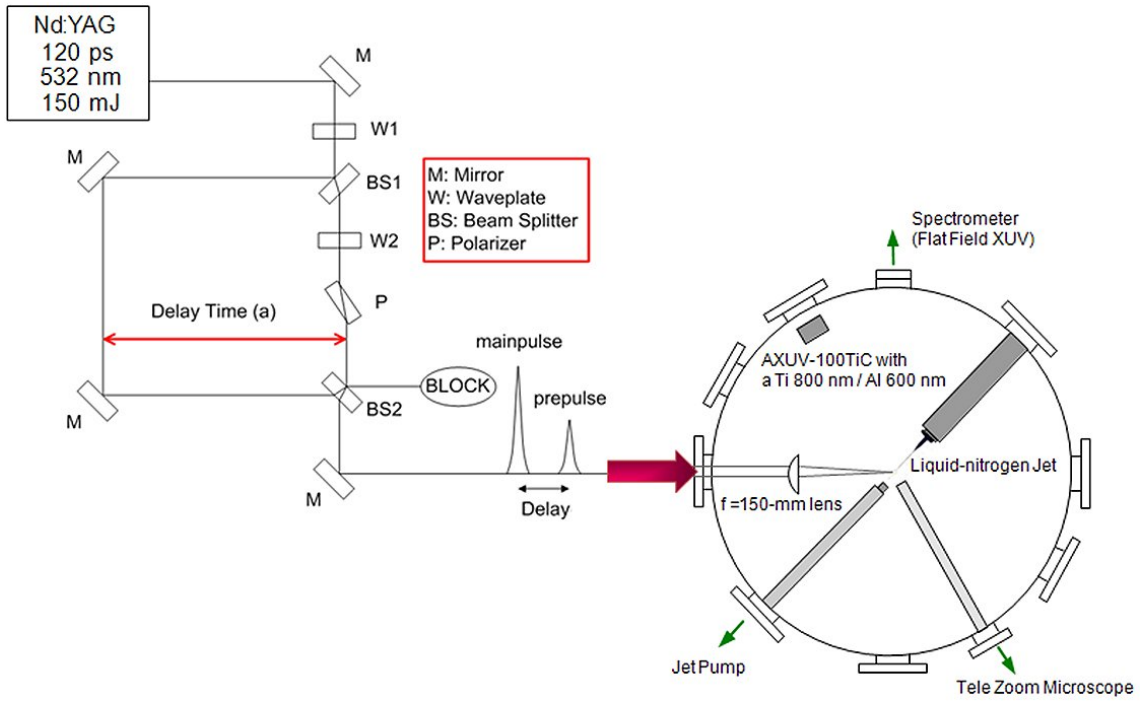

Fig. 2. Schematic experimental setup for the study of the pre-pulse effect. The angle between the jet direction and the laser propagation was 135° due to the experimental arrangement.

W/cm^2.

Figure 1(c) shows the plot of the laser intensities of the maximum conversion efficiency with respect to the pulse duration. The laser intensity of the maximum conversion efficiency decreases as the pulse duration gets longer. The data fitting reveals that $I_m \propto 1/\tau^{\alpha}$, where $\alpha = 0.9 \pm 0.15$.

III. PRE-PULSE EFFECTS

The pre-pulse effect in the case of the liquid-nitrogen jet target is not well known. A systematic investigation of pre-pulse effect in terms of the pre-pulse and the main pulse energy and the delay between two pulses has been carried out. The experimental arrangement is schematically shown in Figure 2. In this study, we used a 13-μm-diameter nozzle to form a 12-μm liquid-nitrogen jet and a 532-nm, 120-ps Nd:YAG laser operating at 10 Hz. The laser was split by using a beam splitter (BS, $R_s = 70$ % and $R_p = 30$ %) into two laser beams. The energies of the laser beams were controlled by rotating the polarization of the laser beams with a wave plate. One beam (main pulse) went through a delay line. The other (pre-pulse) went through another set consisting of a wave plate and a polarizer ($T_s = 0$ % and $T_p = 95$ %), which further controlled the beam energy. The pre-pulse was polarized horizontally to the optical table. The polarization of the main beam was a mixture of horizontal and vertical polarizations, depending on the energy: 15 mJ for pure horizontal polarization, 60 mJ for pure vertical polarization and in between for mixed polarization. These two pulses with intended energies and a delay between them were combined at another BS, forming a train of two pulses. The delay time was varied from 0 to 6 ns. This pulse train was focused by using a $f = 150$-mm lens onto a jet at an angle of 135°, as shown in Figure 2.

Figures 3(a) and (b) show typical quasi-monochromatic spectra and photodiode currents obtained with and without a pre-pulse. The main pulse energy was 60 mJ. The fluctuation of the current signal was less than 10 %. The spectrum clearly showed that the main contribution to the photodiode current came from the 2.88-nm light, indicating that the enhancement of the 2.88-nm light was responsible for the increase of the photodiode current by a factor of about [11].

We investigated the pre-pulse effect by changing the pre-pulse energy, the main pulse energy and the delay between the two pulses. We observed that a higher enhancement in conversion efficiency was achieved for lower main pulse energy. The enhancement at a 1-ns delay was smaller than that at a 6-ns delay, indicating that the 1-ns delay was too short for a proper pre-plasma to be formed. At a 1-ns delay, a 2-mJ pre-pulse energy was not sufficient and at a 6-ns delay, the enhancements were more or less the same as for a pre-pulse energy of $2 - 8$ mJ. Especially, the enhancement in the case of a 15-mJ main pulse was conspicuous [Figure 3(c)]. The results indicate that the main pulse energy is not a critical parameter when the main pulse energy is larger than 30 mJ. The largest

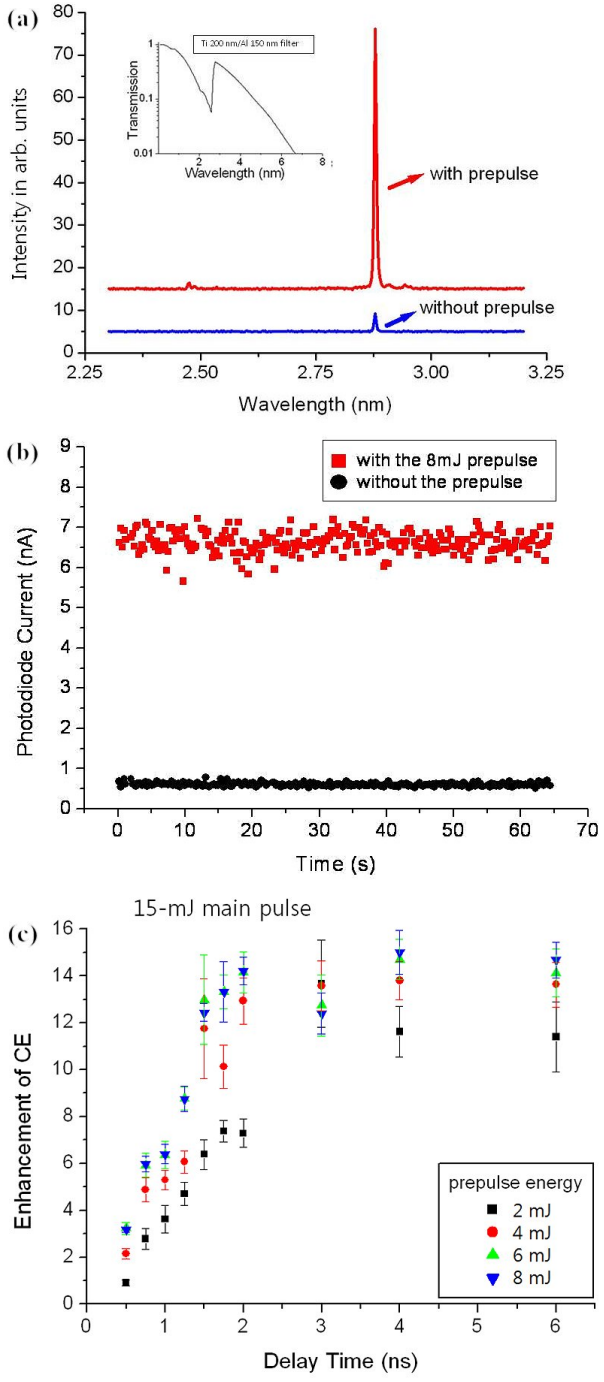

Fig. 3. (a) Spectra and (b) photodiode current with and without the pre-pulse: 60-mJ main pulse, 8-mJ pre-pulse and 6-ns delay. The spectra of the water-window region were obtained with a Ti 200 nm/Al 150 nm filter. The transmission of this filter is shown in the inset of (a). (c) Enhancement of the CE as a function of the pre-pulse energy and the delay time at the 15-mJ main pulse.

enhancement of 14 was observed for a pre-pulse energy of 8 mJ and a main pulse energy of 15 mJ at a delay of 4 ns while for a 60-mJ main pulse energy, an enhancement by a factor of about 10 was obtained. This large enhancement can be understood in terms of the increased inverse-bremsstrahlung absorption due to the expanding pre-plasma's volume enhancement [12].

IV. MULTIPLE PULSE EFFECT

It would be interesting to find out if the radiation would be more than doubled when two pairs of pre-pulse and main pulse are impinged onto a target. The observation of the enhancement would indicate the existence of an optimal temporal structure for a driving pulse. To address this issue, we investigated the multi-pulse effect in the 4-pulse configuration.

The experimental arrangement is schematically shown in Figure 4(a). A 532-nm, 120-ps Nd:YAG laser operating at 10 Hz is split by using a beam splitter 1 (BS1, $R_s \geq 99$ % and $T_p \geq 90$ %) into two laser beams. The energies of the laser beams can be controlled by rotating the polarization of the laser beams with a wave-plate (W1). The reflected beam from BS1 goes through W3 so that the component of the horizontal polarization becomes equal to that of the vertical polarization. BS2 ($R_s \sim 70$ % and $R_p \sim 30$ %) splits the reflected beam from BS1 into two beams (main pulses) having the same energy: the transmitted main pulse1 from BS2 (horizontal component ~70 %, vertical component ~30 %) and the reflected main pulse2 from BS2 (horizontal component ~30 %, vertical component: ~70 %). Undergoing the same process, the transmitted beam from BS1 also generates two beams (pre-pulses) having the same energy: the reflected pre-pulse1 from BS2 (horizontal component ~30 %, vertical component ~70 %) and the transmitted pre-pulse2 from BS2 (horizontal component ~30 %, vertical component ~70 %). The pre-pulse1 and the main pulse1 go through W4 and BS3 ($R_s \geq 99$ % and $T_p \geq 90$ %). The pre-pulse2 and the main pulse2 go through W5 and BS3. If the main pulse1 and the main pulse2 have vertical polarization and horizontal polarization, respectively, by using W4 and W5, we can make the main pulses go through BS3 without losing any energy. However, as the polarizations of the pre-pulse1 and the pre-pulse2 are also changed in the process of using W4 and W5, after passing through the beam splitter3, the pre-pulses lose energy of about 30 %. In doing so, we have pre-pulses of ~6 mJ and main pulses of ~30 mJ. The pre-pulse1 and the main pulse1 are polarized vertically to the optical table and the pre-pulse2 and the main pulse2 are composed of horizontal polarization. With respect to the pre-pulse1, the main pulse1, pre-pulse2, main pulse2 are separated by $2a$, $2b$ and $2a + 2b$, respectively. In the 2-pulse experiment, the enhancement is maximized at a 3- to ~6-ns delay between the two pulses for the case of the 2- to ~8-mJ pre-pulse. The 3-ns delay between a pre-pulse and a main pulse was taken in the current experiment by fixing $a = 45$ cm. By varying the distance b, we could control the delay, $0 \sim 11$ ns, between the

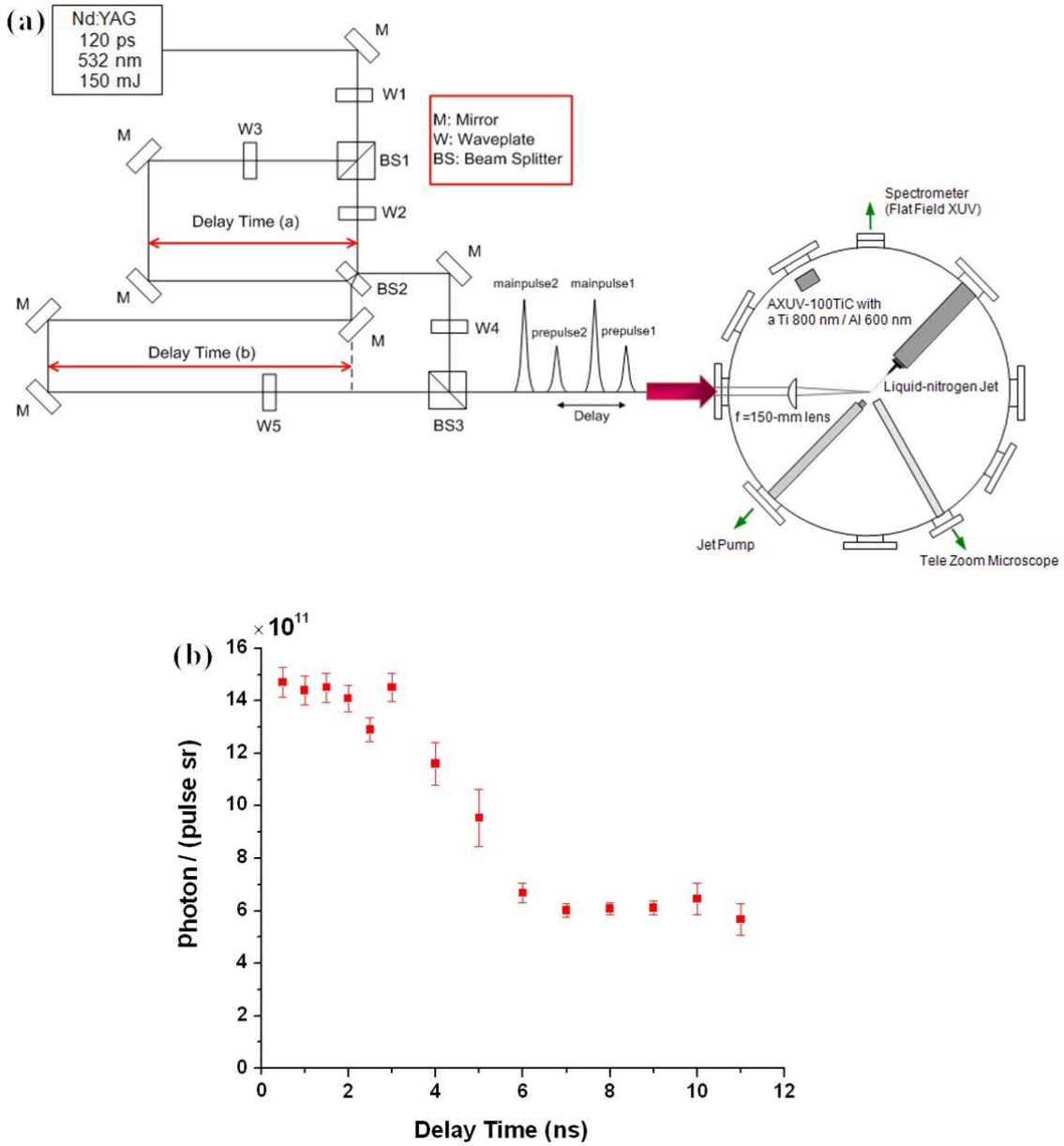

Fig. 4. (a) Schematic experimental setup for the study of the multiple pulse effect. The angle between the jet direction and the laser propagation was 135° due to the experimental arrangement. (b) Photon number as a function of the delay between two pairs of a pre-pulse and a main pulse.

two pairs of pre-pulses and main pulses. This pulse train was focused by using a $f = 150$-mm lens onto a jet at an angle of 135°.

We investigated the multi-pulse effect by changing the delay between the two pairs of pre-pulses and main pulses. Figure 4(b) shows the emitted photon number as a function of the delay time of the two pairs. The enhancement of more than 2 was observed (6-mJ pre-pulse, 30-mJ main pulse). Especially, at a delay of 3 ns, the main pulse1 and the pre-pulse2 were added to result in 3 pulses: 6 mJ (pre-pulse1), 36 mJ (main pulse1 + pre-pulse2), 30 mJ (main pulse2). As shown in Figure 4(b), at 3-ns, the emitted photon number is suddenly increased and 3-pulse structure seems more effective than in the 4-pulse structure. The estimated photon flux is $\sim 1.45 \times 10^{12}$ photons / (pulse sr) at a delay of 0.5- to ~1.5-ns, which is larger by a factor of 2.4 compared to the 2-pulse case.

ACKNOWLEDGMENTS

This work has been supported by the Korean Ministry of Commerce, Industry and Energy, by the National Re-

search Laboratory Program of spell out (KOSEF) and by the BK21 Program of the Korean Research Foundation.

REFERENCES

[1] G. Malka, M. M. Aleonard, J. F. Chemin, G. Claverie, M. R. Harston, J. N. Scheurer, V. Tikhonchuk, S. Fritzler, V. Malka, P. Balcou, G. Grillon, S. Moustaizis, L. Notebaert, E. Lefebvre and N. Cochet, Phys. Rev. E **66**, 066402 (2002).
[2] P. A. C. Jansson, B. A. M. Hansson, O. Hemberg, M. Otendal, A. Holmberg, J. de Groot and H. M. Hertz, Appl. Phys. Lett. **84**, 2256 (2004).
[3] U. Vogt, H. Stiel, I. Will, P. V. Nickles, W. Sandner, M. Wieland and T. Wilhein, Appl. Phys. Lett. **79**, 2336 (2001).
[4] B. A. M. Hansson, L. Rymell, M. Berglund and H. M. Hertz, Microelectron. Eng. **53**, 667 (2000).
[5] G.-M. Zeng, M. Takahashi, H. Daido, T. Kanebe, H. Aritome, M. Nakatsuka and S. Nakai, J. Appl. Phys. **67**, 3597 (1990).
[6] G.-M. Zeng, H. Daido, T. Togawa, M. Nakatsuka and H. Aritome, J. Appl. Phys. **69**, 7460 (1991).
[7] R. C. Spitzer, T. J. Orzechowski, D. W. Phillion, R. L. Kauffman and C. Cerjan, J. Appl. Phys. **77**, 2251 (1995).
[8] R. C. Spitzer, R. L. Kauffman, T. Orzechowski, D. W. Phillion and C. Cerjan, J. Vac. Sci. Technol. B **11**, 2986 (1993).
[9] I. C. E. Turcu, I. N. Ross and G. J. Tallents, Appl. Phys. Lett. **63**, 3046 (1993).
[10] M. J. McCarthy and N. A. Molloy, Chem. Eng. J. **7**, 1 (1974).
[11] AXUV100, International Radiation Detectors, Inc., USA.
[12] M. Berglund, L. Rymell and H. M. Hertz, Appl. Phys. Lett. **69**, 1683 (1996).